

Influence of the mechanical force and the magnetic field on fibre-reinforced medium for three-phase-lag model

Samia M. Said^{a,b} and Mohamed I. A. Othman^{a,c}

^aFaculty of Science, Department of Mathematics, Zagazig University, Zagazig, Egypt; ^bFaculty of Science and Arts, Department of Mathematics, Qassim University, Buridah, Al-mithnab, Saudi Arabia; ^cFaculty of Science, Department of Mathematics, Taif University, Saudi Arabia

ABSTRACT

A new theory of generalised thermoelasticity has been constructed by taking into account the deformation of a fibre-reinforced isotropic thermoelastic medium. A general model of the equations of the formulation in the context of the three-phase-lag model and Green–Naghdi theory without energy dissipation theory are applied to study the influence of a mechanical force, temperature dependent and a magnetic field on the wave propagation within a fibre-reinforced isotropic thermoelastic medium. The exact expressions of the displacement components, temperature and stress components are obtained using normal mode analysis. The variations of the considered variables with the horizontal distance are illustrated graphically for different values of a mechanical force. Comparisons are made between the results of the two theories in the presence and absence of a magnetic field as well as temperature-dependent properties.

ARTICLE HISTORY

Received 29 September 2015
Accepted 30 December 2015

KEYWORDS

Fibre-reinforced; Green–Naghdi theory; magnetic field; mechanical force; three-phase-lag model

1. Introduction

Generalised thermoelasticity theories have been developed with the objective of removing the paradox of an infinite speed of thermal signals inherent in the conventional coupled dynamical theory of thermoelasticity in which parabolic-type heat conduction equation is considered, contradict physical facts. During the last three decades, the generalised theories involving a finite speed of the heat transportation (hyperbolic heat transport equation) in elastic solids have been developed to remove this paradox. The first generalisation is proposed by Lord and Shulman (1967) which involves one thermal relaxation time parameter (single-phase-lag model). The second generalisation of the coupled thermoelasticity theory is developed by Green and Lindsay (1972), which involves two thermal

relaxation times. Experimental studies indicate that the relaxation times can be of relevance in the cases involving a rapidly propagating crack tip, shock wave propagation, laser technique, etc. Because of the experimental evidence in support of finiteness of heat propagation speed, the generalised thermoelasticity theories are considered to be more realistic than the conventional theory in dealing with practical problems involving very large heat fluxes at short intervals like those occurring in laser units and energy channels. The third generalisation is known as low-temperature thermoelasticity introduced by Hetnarski and Ignaczak (1994) called H-I theory. Most engineering materials such as metals possess a relatively high rate of thermal damping and thus are not suitable for use in experiments concerning second sound propagation. But, given the state of recent advances in material science, it may be possible in the foreseeable future to identify (or even manufacture for laboratory purposes) an idealised material for the purpose of studying the propagation of thermal waves at a finite speed. The fourth generalisation is concerned with the thermoelasticity without energy dissipation (TEWOED) and thermoelasticity with energy dissipation (TEWED) introduced by Green and Naghdi (1991, 1992, 1993) and provides sufficient basic modifications in the constitutive equations that permit treatment of a much wider class of heat flow problems, labelled as types I, II, III. The nature of these three types of constitutive equations is such that when the respective theories are linearised, type-I is the same as the classical heat equation (based on Fourier's law) whereas the linearised versions of type-II and type-III theories permit the propagation of thermal waves at a finite speed. The entropy flux vector in type II and III (i.e. TEWOED and TEWED) models are determined in terms of the potential that also determines stresses. When Fourier conductivity is dominant, the temperature equation reduces to classical Fourier law of heat conduction and when the effect of conductivity is negligible the equation has undamped thermal wave solutions without energy dissipation. Applying the above theories of generalised thermoelasticity, several problems have been solved by Bagri and Eslami (2004, 2007a, 2007b), Kar and Kanoria (2007), Roy Choudhuri and Dutta (2005), Ghosh and Kanoria (2008, 2009) etc. The fifth generalisation of the thermoelasticity theory is known as the dual-phase-lag thermoelasticity developed by Tzou (1995) and Chandrasekharaiah (1998). Tzou considered micro-structural effects in the delayed response in time in the macroscopic formulation by taking into account that increase in the lattice temperature is delayed due to photon–electron interactions on the macroscopic level. Tzou (1995) introduced two-phase-lag to both the heat flux vector and the temperature gradient. According to this model, classical Fourier's law $\mathbf{q} = -K\nabla T$ has been replaced by $\mathbf{q}(P, t + \tau_q) = -K\nabla T(P, t + \tau_T)$, where the temperature gradient ∇T at a point P of the material at time $t + \tau_T$ corresponds to the heat flux vector \mathbf{q} at the same point in time $t + \tau_q$. Here K is the thermal conductivity of the material. The delay time τ_T is interpreted as that caused by the micro-structural interactions and is called the phase lag of the temperature gradient. The other delay time τ_q is interpreted as the relaxation time

due to fast-transient effects of thermal inertia. Recently, Roy Choudhuri (2007) introduced the three-phase-lag (3PHL) thermoelasticity which is able to contain all the previous theories at the same time. In this case Fourier's law $\mathbf{q} = -K\nabla T$ has been replaced by $\mathbf{q}(P, t + \tau_q) = -[K\nabla T(P, t + \tau_T) + K^*\nabla v(P, t + \tau_v)]$, where ∇v ($\dot{v} = T$) is the thermal displacement gradient and K^* is the additional material constant and τ_v is the phase lag for the thermal displacement gradient. The purpose of the work of Roy Choudhuri (2007) was to establish a mathematical model that includes three-phase lags in the heat flux vector, the temperature gradient and in the thermal displacement gradient. For this model, we can consider several kinds of Taylor approximations to recover the previously cited theories. In particular, the models of Green and Naghdi are recovered. This theory seems an extension of the one proposed by Tzou (1995). Quintanilla and Racke (2008) studied the stability of solutions for the 3PHL heat conduction. Kar and Kanoria (2009), Abbas (2014), and Kumar and Kumar (2015) have solved different problems applying the 3PHL model.

There are materials which have natural anisotropy such as zinc, magnesium, sapphire, wood, some rocks and crystals, and also there are artificially manufactured materials such as fibre-reinforced composite materials, which exhibit anisotropic character. The advantage of composite materials over the traditional materials lies on their valuable strength, elastic and other properties as Lekhnitskii (1980). A reinforced material may be regarded to some order of an approximation, as homogeneous and anisotropic elastic medium having a certain kind of an elastic symmetry depending on the symmetry of reinforcement. Some glass fibre-reinforced plastics may be regarded as transversely isotropic. The problems of solid mechanics should not be restricted to the isotropic medium only. Increasing use of anisotropic media demands that the study of elastic problems should be extended to anisotropic medium also. Fibre-reinforced composites are widely used in engineering structures, due to their superiority over the structural materials in applications requiring high strength and stiffness in lightweight components. A continuum model is used to explain the mechanical properties of such materials. A reinforced concrete member should be designed for all conditions of stresses that may occur and in accordance with the principles of mechanics. The characteristic property of a reinforced concrete member is that its components, namely concrete and steel, act together as a single unit as long as they remain in the elastic condition, i.e. the two components are bound together so that there can be no relative displacement between them. In the case of an elastic solid reinforced by a series of parallel fibres, it is usual to assume transverse isotropy. In the linear case, the associated constitutive relations, relating infinitesimal stress and strain components have five material constants. In the last three decades, the analysis of the stress and deformation of fibre-reinforced composite materials has been an important research area of solid mechanics. Belfield, Rogers, and Spencer (1983) have introduced the idea of continuous self-reinforcement at every point of an elastic solid. One can find some studies on transversely isotropic elasticity

in the literature (Abd-Alla, Abo-Dahab, & Bayones, 2015; Othman & Atwa, 2014; Othman, Elmaklizi, & Said, 2013; Othman, Lotfy, Said, & Osman, 2012; Sengupta & Nath, 2001; Singh, 2006).

The effect of mechanical and thermal disturbances on an elastic body is studied by the theory of thermoelasticity. This theory has two defects. This theory is studied by Biot (1956). He deals with a defect of the uncoupled theory that mechanical causes have no effect on temperature. The thermal stress in a material with the temperature-dependent properties is studied extensively by Noda (1986). Material properties such as the modulus of the elasticity and thermal conductivity vary with the temperature. When the temperature variation from the initial is not varying high, the properties of materials are constants. In the refractory industries, the structural components are exposed to high temperature change. In this case, neglecting the temperature dependence material properties will be due to errors as Jin and Batra (1998). Ezzat et al. (2004) studied the dependence of the modulus of elasticity on reference temperature in generalised thermoelasticity with thermal relaxation. Othman (2000) and Othman et al. (2013) studied the two-dimensional problem of the generalised thermoelasticity with the temperature-dependent elastic moduli for the different theories. Non-linear transient thermal stress analysis of temperature-dependent hollow cylinders using a finite element model are discussed by Zenkour and Abbas (2014). Fractional order theory of thermoelasticity for elastic medium with temperature-dependent properties are discussed by Wang et al. (2015).

The present paper is concerned with the investigations related to the effect of a mechanical force and a magnetic field for the 3PHL model and TEWOED (G-N II) theory on the plane waves in a fibre-reinforced thermoelastic isotropic medium with temperature-dependent properties. Normal mode analysis is used to obtain the exact expressions for the considered variables. A comparison is carried out between the considered variables in the absence and presence of a magnetic field as well as temperature-dependent properties. A comparison is also made between the results of the two theories for different values of a mechanical force.

2. The governing equations and formulation of the problem

We consider the problem of a thermoelastic half-space ($x \geq 0$). A magnetic field with a constant intensity $H = (0, 0, H_0)$ is acting parallel to the boundary plane (taken as the direction of the z -axis). The surface of a half-space is subjected to a thermal shock which is a function of y and t . We are interested in a plane strain in the xy -plane with displacement vector \mathbf{u} will have the components:

$$u = u(x, y, t), \quad v = v(x, y, t), \quad w = 0. \quad (1)$$

We begin our consideration with linearised electromagnetism equations as in Othman and Said (2013),

$$\underline{J} = \underline{\nabla} \wedge \underline{h} - \epsilon_0 \frac{\partial \underline{E}}{\partial t}, \quad \underline{\nabla} \wedge \underline{E} = -\mu_0 \frac{\partial \underline{h}}{\partial t}, \quad \underline{E} = -\mu_0 (\underline{\dot{u}} \times \underline{H}), \quad \underline{\nabla} \cdot \underline{h} = 0. \quad (2)$$

where μ_0 is the magnetic permeability, ϵ_0 is the electric permeability, \underline{J} is the current density vector, $\underline{\dot{u}}$ is the particle velocity of the medium and the small effect of the temperature gradient on \underline{J} is also ignored.

The constitutive relations and field equations for a fibre-reinforced linearly thermoelastic isotropic medium with respect to the reinforcement direction \mathbf{a} with a hydrostatic initial stress under the influence of the magnetic field and without body forces and heat sources are given by (Belfield et al. 1983; Montanaro, 1999):

(1) The stress–strain relation

$$\sigma_{ij} = \alpha \lambda e_{kk} \delta_{ij} + 2\mu_T e_{ij} + \alpha(a_k a_m e_{km} \delta_{ij} + a_i a_j e_{kk}) + 2(\mu_L - \mu_T)(a_i a_k e_{kj} + a_j a_k e_{ki}) + \beta a_k a_m e_{km} a_i a_j - \gamma \hat{T} \delta_{ij} - P(\omega_{ij} + \delta_{ij}), \quad (3)$$

$$\omega_{ij} = \frac{1}{2}(u_{j,i} - u_{i,j}), \quad e_{ij} = \frac{1}{2}(u_{i,j} + u_{j,i}), \quad e_{kk} = \frac{\partial u}{\partial x} + \frac{\partial v}{\partial y}, \quad i \cdot j = x, y. \quad (4)$$

We assume that as in Othman et al. (2013):

$$\lambda = \lambda_1(1 - \alpha^* T_0), \quad \alpha = \alpha_1(1 - \alpha^* T_0), \quad \mu = \mu_1(1 - \alpha^* T_0), \quad \mu_L = \mu_{L1}(1 - \alpha^* T_0),$$

$$\mu_T = \mu_{T1}(1 - \alpha^* T_0), \quad \gamma = \gamma_1(1 - \alpha^* T_0), \quad \beta = \beta_1(1 - \alpha^* T_0). \quad (5)$$

where $\lambda_1, \alpha_1, \mu_1, \mu_{L1}, \mu_{T1}, \gamma_1, \beta_1$ are the constants of the material and α^* is the linear temperature coefficient.

Introducing Equation (5) in Equation (3), we get

$$\sigma_{xx} = \frac{1}{\alpha_0} [B_{11} u_{,x} + B_{12} v_{,y} - \gamma_1 \hat{T}] - P, \quad (6)$$

$$\sigma_{yy} = \frac{1}{\alpha_0} [B_{12} u_{,x} + B_{22} v_{,y} - \gamma_1 \hat{T}] - P, \quad (7)$$

$$\sigma_{xy} = S_1 u_{,y} + S_2 v_{,x}, \quad \sigma_{yx} = S_2 u_{,y} + S_1 v_{,x}, \quad \sigma_{xz} = \sigma_{yz} = 0. \quad (8)$$

where,

$$B_{11} = \lambda_1 + 2(\alpha_1 + \mu_{T1}) + 4(\mu_{L1} - \mu_{T1}) + \beta_1, \quad B_{12} = \lambda_1 + \alpha_1, \quad B_{22} = \lambda_1 + 2\mu_{T1},$$

$$S_1 = \frac{\mu_{L1}}{\alpha_0} + \frac{P}{2}, \quad S_2 = \frac{\mu_{L1}}{\alpha_0} - \frac{P}{2}, \quad \alpha_0 = \frac{1}{(1 - \alpha^* T_0)}.$$

where σ_{ij} 's are the components of stress, e_{ij} 's are the components of strain, e_{kk} is the dilatation, λ, μ_T 's are the elastic constants, $\alpha, \beta, (\mu_L - \mu_T), \gamma$, are the reinforcement parameters, δ_{ij} is the Kronecker delta, P is the initial pressure, $\hat{T} = T - T_0$, where T is the temperature above the reference temperature T_0 , and $\underline{a} \equiv (a_1, a_2, a_3)$, $a_1^2 + a_2^2 + a_3^2 = 1$. We choose the fibre direction as $\underline{a} \equiv (1, 0, 0)$.

(2) The equation of motion, taking into consideration the Lorentz force, is given by

$$\rho \ddot{u}_i = \sigma_{ij,j} + \mu_0 (\mathbf{J} \times \mathbf{H})_i, \quad i, j = 1, 2, 3. \quad (9)$$

The dynamic displacement vector is actually measured from a steady-state deformed position and the deformation is assumed be small. Due to the application of the initial magnetic field \mathbf{H} , there are an induced magnetic field $\mathbf{h} = (0, 0, h)$ and an induced electric field \mathbf{E} , as well as the simplified equations of electrodynamics of a slowly moving medium for a homogeneous, thermal and electrically conducting, elastic solid. Expressing the components of the vector $\mathbf{J} = (J_1, J_2, J_3)$ in terms of displacement by eliminating the quantities \mathbf{h} and \mathbf{E} from Equation (2), thus yields

$$J_1 = H_0 \left(-\frac{\partial e}{\partial y} + \mu_0 \epsilon_0 \dot{v} \right), \quad J_2 = H_0 \left(\frac{\partial e}{\partial x} - \mu_0 \epsilon_0 \dot{u} \right), \quad J_3 = 0, \quad (10)$$

(3) The generalised heat conduction equation in the 3PHL model is given by Roy Choudhuri (2007)

$$K^* \nabla^2 T + \tau_v^* \nabla^2 \dot{T} + K \tau_T \nabla^2 \ddot{T} = \left(1 + \tau_q \frac{\partial}{\partial t} + \frac{1}{2} \tau_q^2 \frac{\partial^2}{\partial t^2} \right) (\rho C_E \ddot{T} + \gamma T_0 \ddot{e}), \quad (11)$$

where K is the coefficient of thermal conductivity, K^* is the additional material constant, ρ is the mass density, C_E is the specific heat at constant strain, τ_T and τ_q are the phase-lag of temperature gradient and the phase-lag of heat flux, respectively. Also $\tau_v^* = K + \tau_v K^*$, where τ_v is the phase-lag of thermal displacement gradient. In the above equations, a dot denotes the partial derivative with respect to time, and a comma followed by a suffix denotes the partial derivative with respect to the corresponding coordinates.

By substituting from Equations (6)–(8) and (10) in Equation (9) and using the summation convention, we note that the third equation of motion in Equation (9) is identically satisfied and the first two equations become

$$\rho \frac{\partial^2 u}{\partial t^2} = \frac{1}{\alpha_0} \left(B_{11} \frac{\partial^2 u}{\partial x^2} + E_2 \frac{\partial^2 v}{\partial x \partial y} + E_1 \frac{\partial^2 u}{\partial y^2} - \gamma_1 \frac{\partial \hat{T}}{\partial x} \right) - \mu_0 H_0 \frac{\partial h}{\partial x} - \epsilon_0 \mu_0^2 H_0^2 \frac{\partial^2 u}{\partial t^2}, \tag{12}$$

$$\rho \frac{\partial^2 v}{\partial t^2} = \frac{1}{\alpha_0} \left(B_{22} \frac{\partial^2 v}{\partial y^2} + E_2 \frac{\partial^2 u}{\partial x \partial y} + E_1 \frac{\partial^2 v}{\partial x^2} - \gamma_1 \frac{\partial \hat{T}}{\partial y} \right) - \mu_0 H_0 \frac{\partial h}{\partial y} - \epsilon_0 \mu_0^2 H_0^2 \frac{\partial^2 v}{\partial t^2}. \tag{13}$$

where $E_1 = \alpha_0 S_1$, $E_2 = \alpha_1 + \lambda_1 + \alpha_0 S_2$.

Employing Equation (5) and using Equation (11), this yields

$$K^* \nabla^2 T + \tau_v^* \nabla^2 \dot{T} + K \tau_T \nabla^2 \ddot{T} = \left(1 + \tau_q \frac{\partial}{\partial t} + \frac{1}{2} \tau_q^2 \frac{\partial^2}{\partial t^2} \right) \left(\rho C_E \ddot{T} + \frac{\gamma_1}{\alpha_0} T_0 \ddot{\epsilon} \right), \tag{14}$$

Equations (12)–(14) are the field equations of the generalised thermoelasticity elastic solid, applicable to the GN-II theory and 3PHL model as follows:

- (1) Equations of the 3PHL model when, $K, \tau_T, \tau_q, \tau_v > 0$, and the solutions are always (exponentially) stable if $\frac{2K\tau_T}{\tau_q} > \tau_v^* > K^* \tau_q$ as in Quintanilla and Racke (2008)
- (2) Equations of the GN-II theory when, $K = \tau_T = \tau_q = \tau_v = 0$.
- (3) The corresponding equations for a fibre-reinforced linearly thermoelastic isotropic medium with temperature dependence in the presence of a magnetic field for different values of a mechanical force by taking $R_p = 5, 25$.
- (4) The corresponding equations for a fibre-reinforced linearly thermoelastic isotropic medium with temperature dependent in the presence of a mechanical force and without a magnetic field from the above mentioned cases by taking $R_p = 5, H_0 = 0$.
- (5) The corresponding equations for a fibre-reinforced linearly thermoelastic isotropic medium in the presence of a mechanical force and a magnetic field and without temperature dependent from the above mentioned cases by taking $\alpha^* = 0$.

To transform the above equations in non-dimensional forms, we will use the following non-dimensional variables:

$$(x', y', u', v') = c_1 \eta (x, y, u, v), \quad (t', \tau'_q, \tau'_v, \tau'_T) = c_1^2 \eta (t, \tau_q, \tau_v, \tau_T),$$

$$h' = \frac{h}{H_0}, \quad \theta = \frac{\gamma_1 \hat{T}}{(\lambda_1 + 2\mu_{T1})},$$

$$P' = \frac{P}{\mu_{T1}}, \quad \sigma'_{ij} = \frac{\sigma_{ij}}{\mu_{T1}}, \quad i, j = 1, 2. \tag{15}$$

where $\eta = \frac{\rho C_E}{K^*}$, $c_1^2 = \frac{(\lambda_1 + 2\mu_{T1})}{\rho}$.

Using the above non-dimensional variables, then employing $h' = -H_0 e$, Equations (12)–(14) take the following form (dropping the primes for convenience):

$$\alpha_2 \frac{\partial^2 u}{\partial t^2} = L_{11} \frac{\partial^2 u}{\partial x^2} + L_2 \frac{\partial^2 v}{\partial x \partial y} + h_1 \frac{\partial^2 u}{\partial y^2} - \frac{\partial \theta}{\partial x}, \quad (16)$$

$$\alpha_2 \frac{\partial^2 v}{\partial t^2} = L_{22} \frac{\partial^2 v}{\partial y^2} + L_2 \frac{\partial^2 u}{\partial x \partial y} + h_1 \frac{\partial^2 v}{\partial x^2} - \frac{\partial \theta}{\partial y}, \quad (17)$$

$$C_K \theta_{,ii} + C_v \dot{\theta}_{,ii} + C_T \ddot{\theta}_{,ii} = \left(1 + \tau_q \frac{\partial}{\partial t} + \frac{1}{2} \tau_q^2 \frac{\partial^2}{\partial t^2} \right) (\ddot{\theta} + \varepsilon \ddot{\varepsilon}). \quad (18)$$

$$\begin{matrix} w & & h & & e & & r & & e \\ (h_1, h_2, h_{11}, h_{22}, h_0) = \frac{(E_1, E_2, B_{11}, B_{22}, \mu_0 H_0^2)}{\rho c_1^2}, & L_{11} = h_{11} + \alpha_0 H_0, & L_{22} = h_{22} + \alpha_0 H_0, \end{matrix}$$

$$L_2 = h_2 + \alpha_0 h_0 H_0, \quad C_K = \frac{K^*}{\rho C_E c_1^2}, \quad C_v = \frac{\eta K}{\rho C_E} + C_K \tau_v,$$

$$C_T = \frac{\eta K \tau_T}{\rho C_E}, \quad \varepsilon = \frac{\gamma_1^2 T_0}{\rho C_E \alpha_0 (\lambda_1 + 2\mu_{T1})}, \quad \alpha_2 = \alpha_0 \left(1 + \frac{\varepsilon_0 \mu_0^2 H_0^2}{\rho} \right).$$

3. Normal mode analysis

The solution of the considered physical variable can be decomposed in terms of normal modes in the following form:

$$[u, v, \theta, \sigma_{ij}](x, y, t) = [u^*, v^*, \theta^*, \sigma_{ij}^*](x) \exp(\omega t + imy). \quad (19)$$

where, ω is a complex constant, $i = \sqrt{-1}$, m is the wave number in the y -direction and $u^*(x)$, $v^*(x)$, $\theta^*(x)$, and $\sigma_{ij}^*(x)$ are the amplitudes of the field quantities.

Introducing Equation (19) in Equations (16)–(18), we get

$$[L_{11} D^2 - A_1] u^* + im L_2 D v^* = D \theta^*, \quad (20)$$

$$im L_2 D u^* + [h_1 D^2 - A_2] v^* = im \theta^*, \quad (21)$$

$$A_3 D u^* + i m A_3 v^* = [A_4 D^2 - A_5] \theta^*, \quad (22)$$

where,

$$A_1 = \alpha_2 \omega^2 + h_1 m^2, \quad A_2 = \alpha_2 \omega^2 + L_{22} m^2, \quad A_3 = \varepsilon \omega^2 \left(1 + \tau_q \omega + \frac{1}{2} \tau_q^2 \omega^2 \right),$$

$$A_4 = C_K + C_v \omega + C_T \omega^2, \quad A_5 = A_4 m^2 + A_3 / \varepsilon, \quad D = \frac{d}{dx}.$$

Eliminating $v^*(x)$ and $\theta^*(x)$ between Equations (20)–(22), we obtain the sixth-order ordinary differential equation satisfied with $u^*(x)$,

$$[D^6 - A D^4 + B D^2 - C] u^*(x) = 0, \quad (23)$$

where,

$$A = \frac{1}{h_1 L_{11} A_4} \{ h_1 A_3 - m^2 L_2^2 A_4 + h_1 L_{11} A_5 + L_{11} A_2 A_4 + h_1 A_1 A_4 \},$$

$$B = \frac{1}{h_1 L_{11} A_4} \{ A_3 A_2 + h_1 A_1 A_5 + A_1 A_2 A_4 + L_{11} m^2 A_3 + L_{11} A_2 A_5 - 2 m^2 L_2 A_3 - m^2 L_2^2 A_5 \},$$

$$C = \frac{1}{h_1 L_{11} A_4} \{ m^2 A_1 A_3 + A_1 A_2 A_5 \}.$$

Equation (23) can be factored as

$$(D^2 - k_1^2) (D^2 - k_2^2) (D^2 - k_3^2) u^*(x) = 0, \quad (24)$$

where $k_n^2 (n = 1, 2, 3)$ are the roots of the characteristic Equation of (23).

The solution of Equation (23), which is bound as $x \rightarrow \infty$, is given by

$$u^*(x) = \sum_{n=1}^3 G_n \exp(-k_n x). \quad (25)$$

Similarly,

$$v^*(x) = \sum_{n=1}^3 H_{1n} G_n \exp(-k_n x), \quad (26)$$

$$\theta^*(x) = \sum_{n=1}^3 H_{2n} G_n \exp(-k_n x). \quad (27)$$

$$\text{where } H_{1n} = \frac{im[A_1+(L_2-L_1)k_n^2]}{h_1k_n^3-(A_2-m^2L_2)k_n}, \quad H_{2n} = \frac{-L_1k_n^2+A_1+imL_2k_nH_{1n}}{k_n}.$$

Using Equations (15) and (19) in Equations (6)–(8), we obtain

$$\sigma_{xx}^* = \frac{1}{\alpha_0\mu_{T1}} [B_{11} D u^* + im B_{12} v^* - (\lambda_1 + 2\mu_{T1}) \theta^*] - P^*, \quad (28)$$

$$\sigma_{yy}^* = \frac{1}{\alpha_0\mu_{T1}} [B_{12} D u^* + im B_{22} v^* - (\lambda_1 + 2\mu_{T1}) \theta^*] - P^*, \quad (29)$$

$$\sigma_{xy}^* = \frac{1}{\mu_{T1}} [im S_1 u^* + D S_2 v^*], \quad (30)$$

Introducing Equations (25)–(27) in Equations (28)–(30), this yields

$$\sigma_{xx}^* = \sum_{n=1}^3 H_{3n} G_n \exp(-k_n x) - P^*, \quad (31)$$

$$\sigma_{yy}^* = \sum_{n=1}^3 H_{4n} G_n \exp(-k_n x) - P^*, \quad (32)$$

$$\sigma_{xy}^* = \sum_{n=1}^3 H_{5n} G_n \exp(-k_n x), \quad (33)$$

where,

$$P^* = P \exp[-(\omega t + imy)], \quad H_{3n} = \frac{1}{\alpha_0\mu_{T1}} [-B_{11}k_n + imB_{12}H_{1n} - (\lambda_1 + 2\mu_{T1})H_{2n}],$$

$$H_{4n} = \frac{1}{\alpha_0\mu_{T1}} [-B_{12}k_n + imB_{22}H_{1n} - (\lambda_1 + 2\mu_{T1})H_{2n}], \quad H_{5n} = \frac{1}{\mu_{T1}} [im S_1 - S_2k_nH_{1n}].$$

4. Application

In this section we determine the parameters G_n ($n = 1, 2, 3$). In the physical problem, we should suppress the positive exponentials that are unbounded at infinity. The constants G_1, G_2, G_3 have to be chosen such that the boundary conditions on the surface at $x = 0$ take the form,

- (1) A thermal boundary condition that the surface of the half-space is subjected to a thermal insulated boundary,

$$\frac{\partial \theta}{\partial x} = 0. \quad (34)$$

- (2) Mechanical boundary condition that the surface of the half-space is subjected to a mechanical force,

$$\sigma_{xx} = f(0, y, t) = -R_p f^* e^{\omega t + i m y} - P. \quad (35)$$

- (3) Mechanical boundary condition that the surface of the half-space is subjected to traction free,

$$\sigma_{xy}(0, y, t) = 0. \quad (36)$$

where $f(y, t)$ is an arbitrary function, f^* is a constant and R_p is the magnitude of mechanical force. Substituting the expressions of the variables considered into the above boundary conditions Equations (34)–(36), we can obtain the following equations satisfied by the parameters:

$$-\sum_{n=1}^3 k_n H_{2n} G_n = 0, \quad \sum_{n=1}^3 H_{3n} G_n = -R_p f^*, \quad \sum_{n=1}^3 H_{5n} G_n = 0. \quad (37)$$

By solving the above system of Equation (37), we obtain a system of three equations. After applying the inverse of matrix method, we have the values of the three constants $G_n (n = 1, 2, 3)$. Hence, we obtain the expressions of displacements, temperature distribution, and the stress components.

$$\begin{bmatrix} G_1 \\ G_2 \\ G_3 \end{bmatrix} = \begin{bmatrix} k_1 H_{21} & k_2 H_{22} & k_3 H_{23} \\ H_{31} & H_{32} & H_{33} \\ H_{51} & H_{52} & H_{53} \end{bmatrix}^{-1} \begin{bmatrix} 0 \\ -R_p f^* \\ 0 \end{bmatrix}. \quad (38)$$

5. Numerical results and discussion

With a view to illustrating the analytical procedure presented earlier, we now consider a numerical example for which computational results are given, to compare these in the context of the 3PHL model and the GN-II theory, and to study the effect of a magnetic field and a mechanical force on the wave propagation in a conducting fibre-reinforcement, we now present some numerical results for the physical constants as the follows:

$$\begin{aligned} \lambda_1 &= 7.59 \times 10^9 \text{ N} \cdot \text{m}^{-2}, \quad \mu_{T1} = 1.89 \times 10^{10} \text{ N m}^{-2}, \\ \mu_{L1} &= 2.45 \times 10^{10} \text{ N m}^{-2}, \quad \rho = 7800 \text{ kg} \cdot \text{m}^{-3}, \end{aligned}$$

$$P = 1 \text{ N.K.m}^{-2}, \alpha_1 = -1.28 \times 10^{10} \text{ N.m}^{-2}, \beta_1 = .32 \times 10^{10} \text{ N.m}^{-2},$$

$$T_0 = 300 \text{ K}, \alpha^* = .008 \text{ K}^{-1},$$

$$C_E = 383.1 \text{ J.kg}^{-1} \text{ K}^{-1}, \tau_q = .009 \text{ s}, \tau_v = .006 \text{ s},$$

$$\alpha_t = 8.78 \times 10^{-5} \text{ K}^{-1}, K^* = 386 \text{ ws}^{-1} \text{ m}^{-1} \text{ K}^{-1},$$

$$\mu_1 = 3.86 \times 10^{10} \text{ kg m}^{-1} \text{ s}^{-2}, f^* = 1, K = 120 \text{ w m}^{-1} \text{ K}^{-1},$$

$$\omega = \omega_0 + i\xi, \omega_0 = 1, \xi = .3,$$

$$m = .8, \mu_0 = 1.9, \varepsilon_0 = .7, H_0 = 80, \tau_T = .007 \text{ s}.$$

The computations were carried out for a value of time $t = .2$. The variations of the thermal temperature θ , the displacement components u, v , and the stress components $\sigma_{xx}, \sigma_{yy}, \sigma_{xy}$ with distance x in the plane $y = .5$ for the problem under consideration based on the 3PHL model and the G-N II theory. The results are shown in Figures 1–18. The graphs show four curves predicted by two different theories of thermoelasticity. In these figures, the solid lines represent the solution in the 3PHL model and the dashed lines represent the solution derived using the G-N II theory. Here, all the variables are taken in non-dimensional forms and we consider five cases.

Figures 1–6 show comparisons between the displacement components u, v , the temperature θ , and the stress components $\sigma_{xx}, \sigma_{yy}, \sigma_{xy}$ with temperature-dependent properties in the presence of a magnetic field for different values of mechanical force ($R_p = 5, 25$).

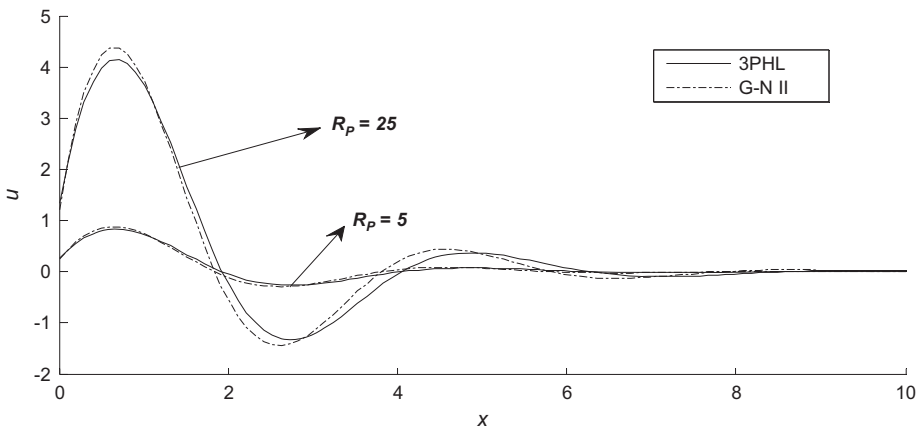


Figure 1. Horizontal displacement distribution u for different values of a mechanical force.

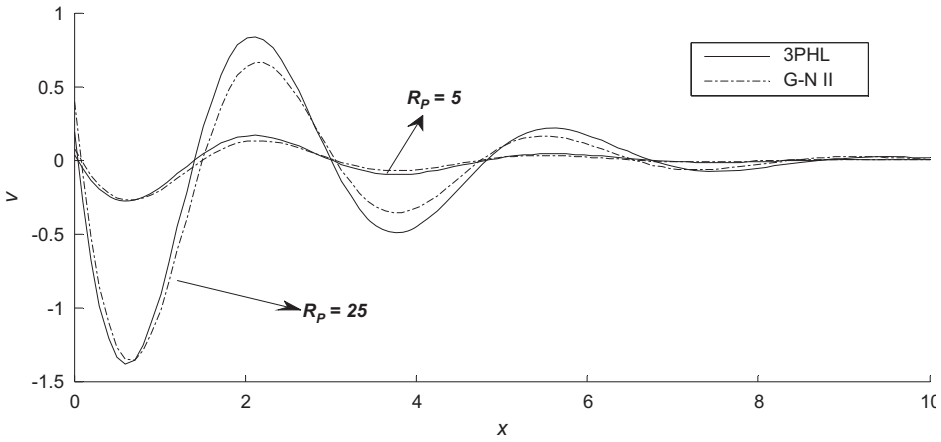


Figure 2. Vertical displacement distribution v for different values of a mechanical force.

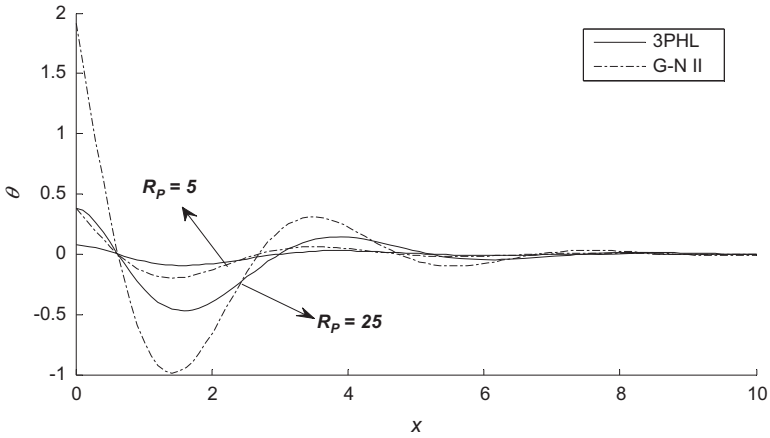


Figure 3. Temperature distribution θ for different values of a mechanical force.

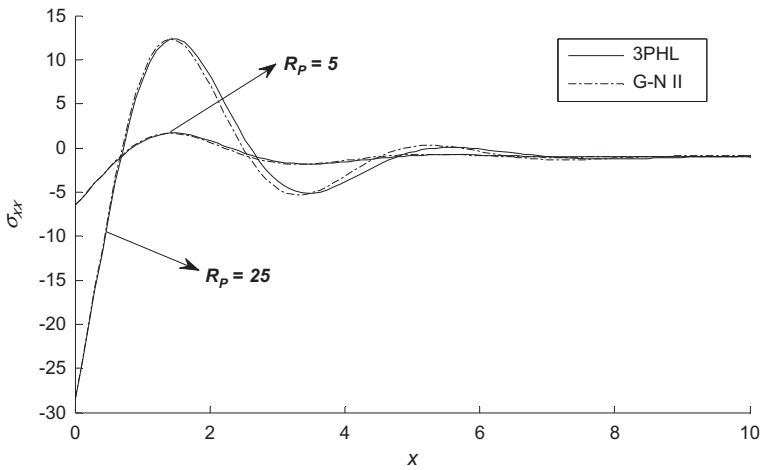


Figure 4. Distribution of stress component σ_{xx} for different values of a mechanical force.

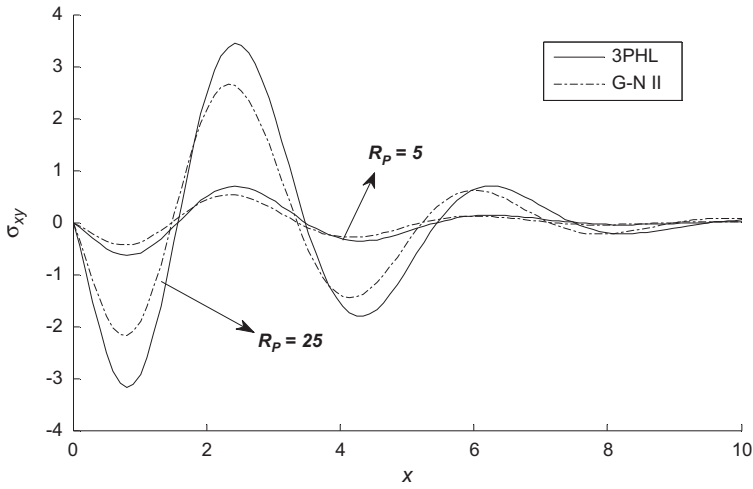


Figure 5. Distribution of stress component σ_{xy} for different values of a mechanical force.

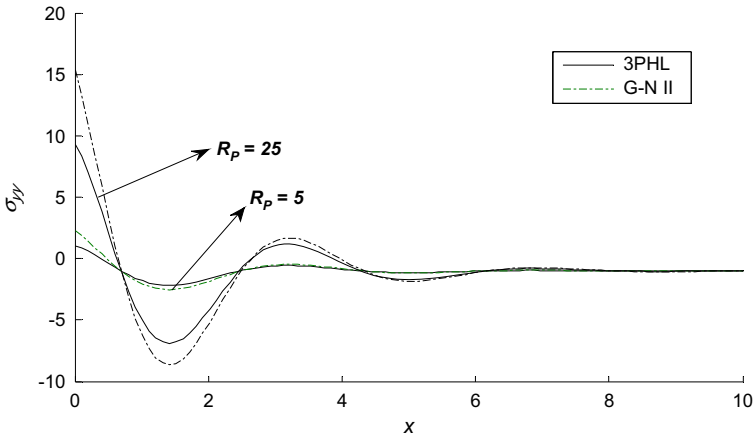


Figure 6. Distribution of stress component σ_{yy} for different values of a mechanical force.

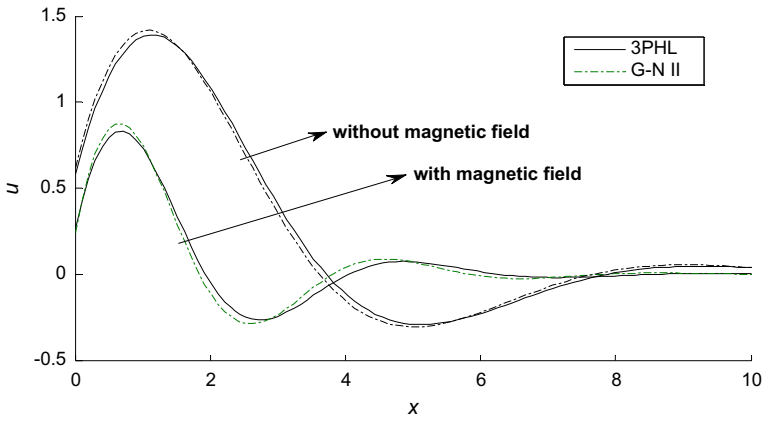


Figure 7. Horizontal displacement distribution u in the absence and presence of a magnetic field.

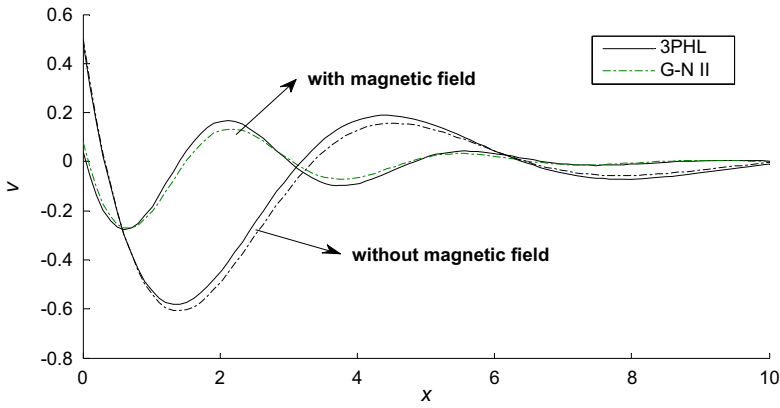


Figure 8. Vertical displacement distribution v in the absence and presence of a magnetic field.

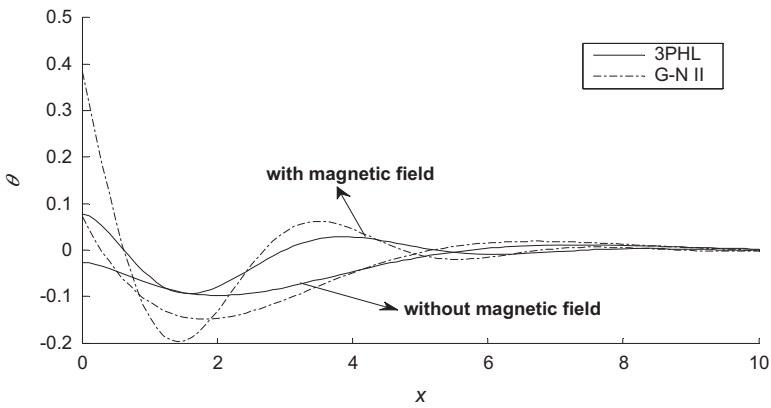


Figure 9. Temperature distribution θ in the absence and presence of a magnetic field.

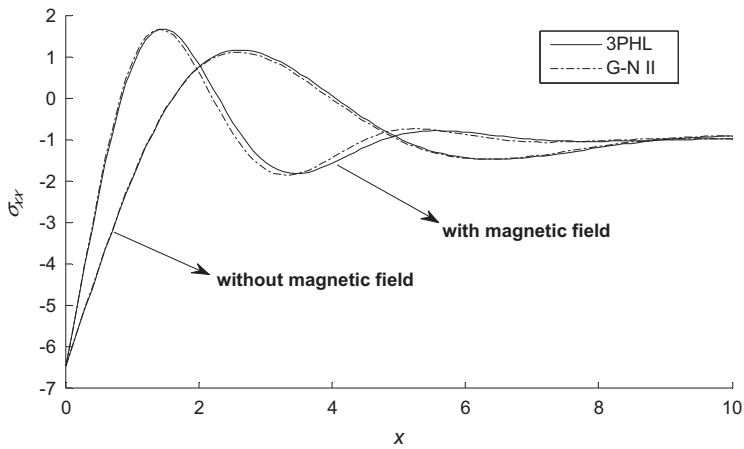


Figure 10. Distribution of stress component σ_{xx} in the absence and presence of a magnetic field.

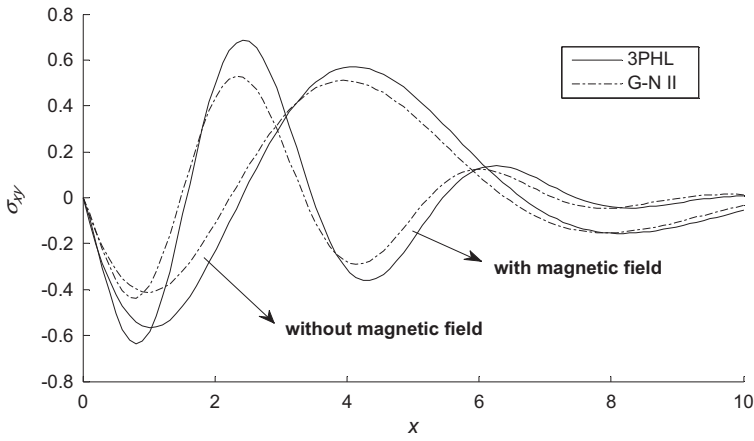


Figure 11. Distribution of stress component σ_{xy} in the absence and presence of a magnetic field.

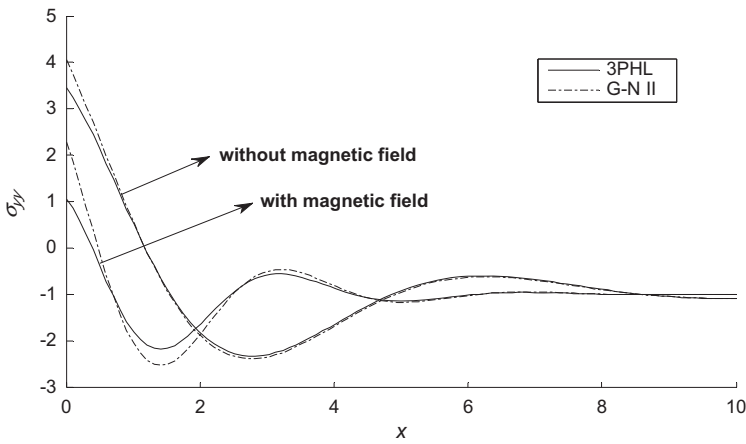


Figure 12. Distribution of stress component σ_{yy} in the absence and presence of a magnetic field.

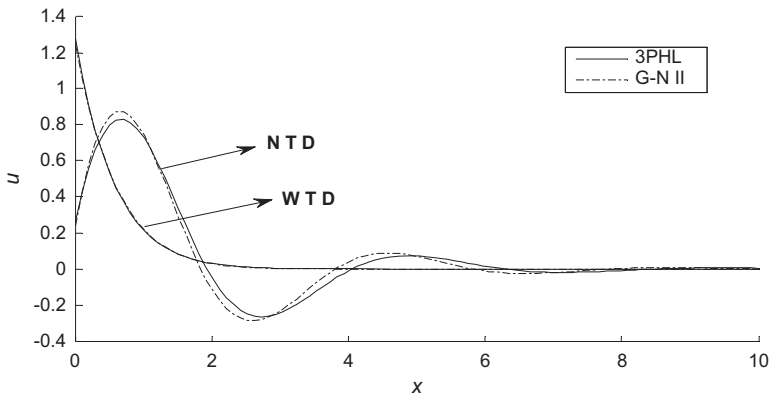


Figure 13. Horizontal displacement distribution u for dependent and independent temperature.

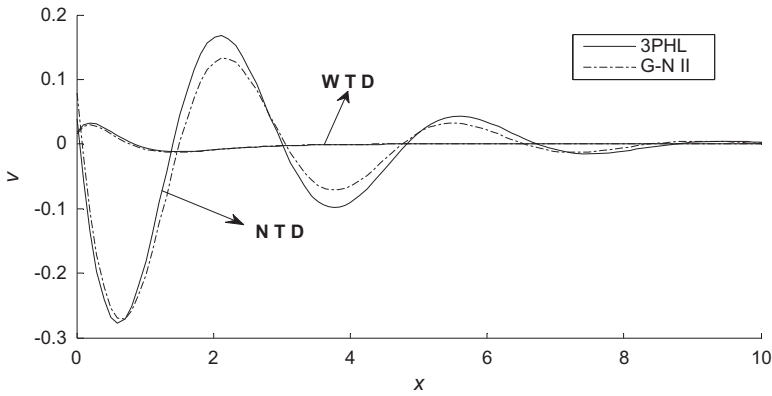


Figure 14. Vertical displacement distribution v for dependent and independent temperature.

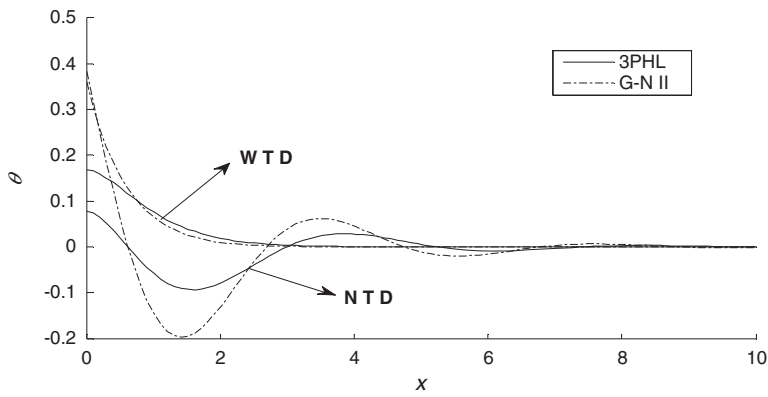


Figure 15. Temperature distribution θ for dependent and independent temperature.

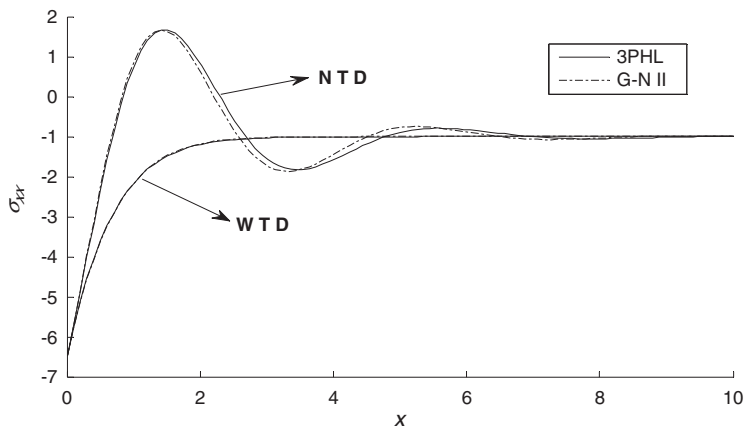


Figure 16. Distribution of stress component σ_{xx} for dependent and independent temperature.

Figure 1 depicts that the distribution of the horizontal displacement u begins from positive values. In the context of the two theories, u starts with increasing to a maximum value in the range $0 \leq x \leq 1$, then decreases to a minimum value in the range $1 \leq x \leq 2.8$, and also moves in a wave propagation for $R_p = 25$. However, in the context of the two theories, u starts with increasing to a maximum value in the range $0 \leq x \leq 1$, then decreases to a minimum value in the range $1 \leq x \leq 3$, and then becomes nearly constant for $R_p = 5$. Figure 2 shows that the distribution of the vertical displacement v begins from positive values. In the context of the two theories, v starts with decreasing to a minimum value in the range $0 \leq x \leq .8$, then increases to a maximum value, and also moves in a wave propagation for $R_p = 25, 5$. Figure 3 exhibits that the distribution of the temperature θ , in the context of the two theories, starts with decreasing in the range $0 \leq x \leq 1.6$, then increases, and in the last becomes nearly constant for $R_p = 5$. However, in the context of the two theories, θ starts with decreasing to a minimum value, then increases, and also moves in a wave propagation for $R_p = 25$. Figure 4 displays that the distribution of the stress component σ_{xx} begins from negative values

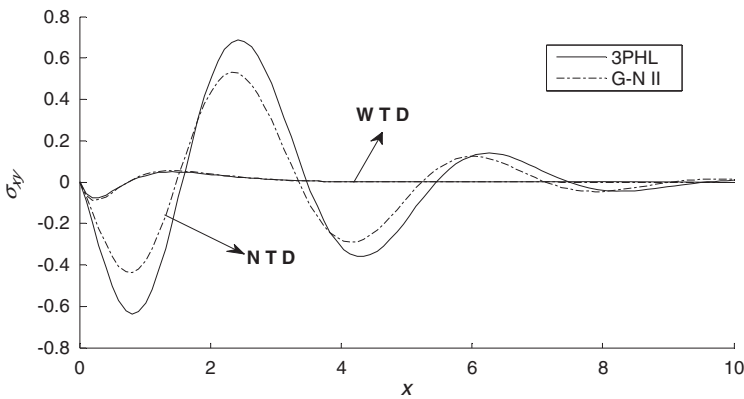


Figure 17. Distribution of stress component σ_{xy} for dependent and independent temperature.

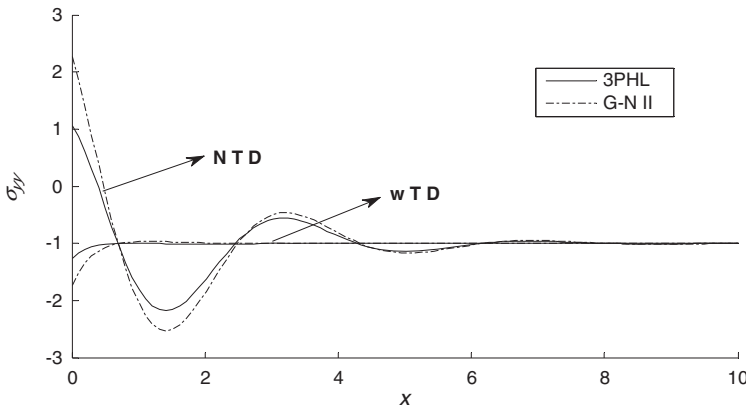


Figure 18. Distribution of stress component σ_{yy} for dependent and independent temperature.

and satisfies the boundary condition at $x = 0$. In the context of the two theories, σ_{xx} starts with increasing to a maximum value in the range $0 \leq x \leq 1.8$, then decreases, and also moves in a wave propagation for $R_p = 25$. However, in the context of the two theories, σ_{xx} starts with increasing to a maximum value in the range $0 \leq x \leq 1.5$, then decreases, and in the last becomes nearly constant for $R_p = 5$. Figure 5 explains the distribution of the stress component σ_{xy} and demonstrates that it reaches a zero value and satisfies the boundary condition at $x = 0$. In the context of the two theories, σ_{xy} starts with decreasing to a minimum value in the range $0 \leq x \leq 1$, then increases to a maximum value, and also moves in a wave propagation for $R_p = 5, 25$. Figure 6 depicts that the distribution of the stress component σ_{yy} , in the context of the two theories, starts with decreasing to a minimum value in the range $0 \leq x \leq 1.8$, then increases, and also moves in a wave propagation for $R_p = 25$. However, in the context of the two theories, σ_{yy} starts with decreasing to a minimum value in the range $0 \leq x \leq 1.5$ then increases, and in the last becomes nearly constant for $R_p = 5$.

Figures 7–12 show comparisons between the displacement components u, v , the temperature θ , and the stress components $\sigma_{xx}, \sigma_{yy}, \sigma_{xy}$, with temperature-dependent properties in the absence ($H_0 = 0$) and presence ($H_0 = 80$) of a magnetic field with a mechanical force ($R_p = 5$).

Figure 7 depicts that the distribution of the horizontal displacement u begins from positive values. In the context of the two theories, u starts with increasing to a maximum value in the range $0 \leq x \leq 1.8$, then decreases to a minimum value, and again increases for $H_0 = 0$. Figure 8 shows that the distribution of the vertical displacement v begins from positive values. In the context of the two theories, v starts with decreasing to a minimum value in the range $0 \leq x \leq 1.7$, then increases, and again decreases for $H_0 = 0$. Figure 9 exhibits that the distribution of the temperature θ , in the context of the two theories, θ starts with decreasing to a minimum value in the range $0 \leq x \leq 1.8$, then increases, and again decreases for $H_0 = 0$. Figure 10 explains that the distribution of the stress component σ_{xx} begins from a negative value and satisfies the boundary condition at $x = 0$. In the context of the two theories, σ_{xx} starts with increasing to a maximum value in the range $0 \leq x \leq 2.6$, then decreases, and again increases for $H_0 = 0$. Figure 11 displays the distribution of the stress component σ_{xy} and demonstrates that it reaches a zero value and satisfies the boundary condition at $x = 0$. In the context of the two theories, σ_{xy} starts with decreasing to a minimum value in the range $0 \leq x \leq 1$, then increases to a maximum value, and also moves in a wave propagation for $H_0 = 0$. Figure 12 depicts that the distribution of the stress component σ_{yy} begins from positive value. In the context of the two theories, σ_{yy} starts with decreasing to a minimum value in the range $0 \leq x \leq 3$, then increases, and again decreases for $H_0 = 0$.

Figures 13–18 show comparisons between the displacement components u, v , the temperature θ , and the stress components $\sigma_{xx}, \sigma_{yy}, \sigma_{xy}$, with (N T D) and without (W T D) temperature-dependent properties in the presence of a magnetic field for $R_p = 5$.

Figure 13 depicts that the distribution of the horizontal displacement u begins from positive values. In the context of the two theories, u decreases in the range $0 \leq x \leq 10$ for W T D. Figure 14 shows that the distribution of the vertical displacement v begins from positive values. In the context of the two theories, v starts with increasing to a maximum value in the range $0 \leq x \leq .2$, then decreases, and in the last becomes nearly constant for W T D. Figure 15 explains that the distribution of the temperature θ begins from positive values. In the context of the two theories, θ decreases in the range $0 \leq x \leq 10$ for W T D. Figure 16 exhibits that the distribution of the stress component σ_{xx} begins from a negative value and satisfies the boundary condition at $x = 0$. In the context of the two theories, σ_{xx} starts with increasing in the range $0 \leq x \leq 3$, and then becomes nearly constant for W T D. Figure 17 displays the distribution of the stress component σ_{xy} and demonstrates that it reaches a zero value and satisfies the boundary condition at $x = 0$. In the context of the two theories, σ_{xy} starts with decreasing to a minimum value in the range $0 \leq x \leq .3$, then increases, and in the last becomes nearly constant for W T D. Figure 18 depicts that the distribution of the stress component σ_{yy} , in the context of the two theories, starts with increasing, and then becomes nearly constant for W T D.

6. Conclusion

In the present study, normal mode analysis is used to study the effect of a mechanical force and a magnetic field on a fibre-reinforced thermoelastic medium based on the 3PHL model and GN-II theory. We obtain the following conclusions based on the above analysis:

- (1) The phase-lag of the temperature gradient, the phase-lag of the thermal displacement gradient and the phase-lag of heat flux have significant effects on all the field quantities.
- (2) The mechanical force R_p , the magnetic field (H_0) and the temperature (α^*) have a significant effect on all the field quantities.
- (3) Deformation of a body depends on the nature of the applied force as well as the type of boundary conditions.
- (4) The method that was used in the present article is applicable to a wide range of problems in hydrodynamics and thermoelasticity.
- (5) Analytical solutions based upon normal mode analysis of the thermoelastic problem in solids have been developed and utilised.
- (6) 3PHL model is the most adequate theory to describe the present problem.

Disclosure statement

No potential conflict of interest was reported by the authors.

Funding

This work was supported by the Zagazig University.

References

- Abbas, I. A. (2014). Three-phase lag model on thermoelastic interaction in an unbounded fiber-reinforced anisotropic medium with a cylindrical cavity. *Journal of Computational and Theoretical Nanoscience*, 11, 987–992.
- Abd-Alla, A. M., Abo-Dahab, S. M., & Bayones, F. S. (2015). Wave propagation in fibre-reinforced anisotropic thermoelastic medium subjected to gravity field. *Structural Engineering and Mechanics*, 53, 277–296.
- Bagri, A., & Eslami, M. R. (2004). Generalized coupled thermoelasticity of disks based on the Lord–Shulman model. *Journal of Thermal Stresses*, 27, 691–704.
- Bagri, A., & Eslami, M. R. (2007a). Analysis of thermoelastic waves in functionally graded hollow spheres based on the Green-Lindsay theory. *Journal of Thermal Stresses*, 30, 1175–1193.
- Bagri, A., & Eslami, M. R. (2007b). A unified generalized thermoelasticity formulation; application to thick functionally graded cylinders. *Journal of Thermal Stresses*, 30, 911–930.
- Belfield, A. J., Rogers, T. G., & Spencer, A. J. M. (1983). Stress in elastic plates reinforced by fibres lying in concentric circles. *Journal of the Mechanics and Physics of Solids*, 31, 25–54.
- Biot, M. A. (1956). Thermoelasticity and irreversible thermodynamics. *Journal of Applied Physics*, 27, 240–253.
- Chandrasekharaiah, D. S. (1998). Hyperbolic thermoelasticity: A review of recent literature. *Applied Mechanics Reviews*, 51, 8–16.
- Ezzat, M. A., El-Karamany, A., & Samaan, A. A. (2004). The dependence of the modulus of elasticity on reference temperature in generalized thermoelasticity with thermal relaxation. *Applied Mathematics and Computation*, 147, 169–189.
- Ghosh, M. K., & Kanoria, M. (2008). Generalized thermoelastic problem of a spherically isotropic infinite elastic medium containing a spherical cavity. *Journal of Thermal Stresses*, 31, 665–679.
- Ghosh, M. K., & Kanoria, M. (2009). Analysis of thermoelastic response in a functionally graded spherically isotropic hollow sphere based on Green-Lindsay theory. *Acta Mechanica*, 207, 51–67.
- Green, A. E., & Lindsay, K. A. (1972). Thermoelasticity. *Journal of Elasticity*, 2, 1–7.
- Green, A. E., & Naghdi, P. M. (1991). A re-examination of the basic postulates of thermomechanics. *Proceedings of the Royal Society A: Mathematical, Physical and Engineering Sciences*, 432, 171–194.
- Green, A. E., & Naghdi, P. M. (1992). On undamped heat waves in an elastic solid. *Journal of Thermal Stresses*, 15, 253–264.
- Green, A. E., & Naghdi, P. M. (1993). Thermoelasticity without energy dissipation. *Journal of Elasticity*, 31, 189–208.
- Hetnarski, R. B., & Ignaczak, J. (1994). Generalized thermoelasticity: Response of semi-space to a short laser pulse. *Journal of Thermal Stresses*, 17, 377–396.
- Jin, Z. H., & Batra, R. C. (1998). Thermal fracture of ceramics with temperature-dependent properties. *Journal of Thermal Stresses*, 21, 157–176.
- Kar, A., & Kanoria, M. (2007). Thermo-elastic interaction with energy dissipation in an unbounded body with a spherical hole. *International Journal of Solids and Structures*, 44, 2961–2971.

- Kar, A., & Kanoria, M. (2009). Generalized thermo-visco-elastic problem of a spherical shell with three-phase-lag effect. *Applied Mathematical Modelling*, 33, 3287–3298.
- Kumar, A., & Kumar, R. (2015). A domain of influence theorem for thermoelasticity with three-phase-lag model. *Journal of Thermal Stresses*, 38, 744–755.
- Lekhnitskii, S. (1980). *Theory of elasticity of an anisotropic body*. Moscow: Mir.
- Lord, H. W., & Shulman, Y. (1967). A generalized dynamical theory of thermoelasticity. *Journal of the Mechanics and Physics of Solids*, 15, 299–309.
- Montanaro, A. (1999). On singular surfaces in isotropic linear thermoelasticity with initial stress. *The Journal of the Acoustical Society of America*, 106, 1586–1588.
- Noda, N. (1986). Thermal Stresses in materials with temperature-dependent properties. In R. B. Hetnaraski (Ed.), *Thermal stresses I* (pp. 391–483). North-Holland, Amsterdam.
- Othman, M. I. A. (2000). Lord-Shulman theory under the dependence of the modulus of elasticity on the reference temperature in two dimensional generalized thermoelasticity. *Journal of Thermal Stresses*, 25, 1027–1045.
- Othman, M. I. A., & Atwa, S. Y. (2014). Effect of rotation on a fiber-reinforced thermo-elastic under Green–Naghdi theory and influence of gravity. *Meccanica*, 49, 23–36.
- Othman, M. I. A., & Said, S. M. (2013). Plane waves of a fiber-reinforcement magneto-thermoelastic comparison of three different theories. *International Journal of Thermophysics*, 34, 366–383.
- Othman, M. I. A., Lotfy, Kh., Said, S. M., & Osman, B. (2012). Wave propagation of fiber-reinforced micropolar thermoelastic medium with voids under three theories. *Journal of Applied Mathematics and Mechanics*, 8, 52–69.
- Othman, M. I. A., Elmaklizi, Y. D., & Said, S. M. (2013). Generalized thermoelastic medium with temperature-dependent properties for different theories under the effect of gravity field. *International Journal of Thermophysics*, 34, 521–537.
- Quintanilla, R., & Racke, R. (2008). A note on stability in three-phase-lag heat conduction. *International Journal of Heat and Mass Transfer*, 51, 24–29.
- Roy Choudhuri, S. K. (2007). On a thermoelastic three-phase-lag model. *Journal of Thermal Stresses*, 30, 231–238.
- Roy Choudhuri, S. K., & Dutta, P. S. (2005). Thermoelastic interaction without energy dissipation in an infinite solid with distributed periodically varying heat sources. *International Journal of Solids and Structures*, 42, 4192–4203.
- Sengupta, P. R., & Nath, S. (2001). Surface waves in fibre-reinforced anisotropic elastic media. *Sādhanā*, 26, 363–370.
- Singh, B. (2006). Wave propagation in thermally conducting linear fibre-reinforced composite materials. *Archive of Applied Mechanics*, 75, 513–520.
- Tzou, D. Y. (1995). A unified field approach for heat conduction from macro- to micro-scales. *Journal of Heat Transfer*, 117, 8–16.
- Wang, Y. Z., Liu, D., Wang, Q., & Zhou, J. Z. (2015). Fractional order theory of thermoelasticity for elastic medium with variable material properties. *Journal of Thermal Stresses*, 38, 665–676.
- Zenkour, A. M., & Abbas, I. A. (2014). Nonlinear transient thermal stress analysis of temperature-dependent hollow cylinders using a finite element model. *International Journal of Structural Stability and Dynamics*, 14, 1–17.